Pergamon

PII: S0191-8141(97)00014-X

Journal of Structural Geology, Vol. 19, No. 6, pp. 887 to 892, 1997

0191-8141/97 $17.00 + 0.00

Brevia

SHORT NOTE

A Mohr circle construction for the opening of a pre-existing fracture

R. J. H. JOLLY* and D. J. SANDERSON

Geomechanics Research Group, Department of Geology, University of Southampton, Southampton, U.K.

(*Received* 3 *July* 1996; *accepted in revised form* 17 *January* 1997)

Abstract—The opening of a fracture is dependent on the fluid pressure and the local stress regime around the fracture. For a fracture to open, the fluid pressure must exceed the normal stress acting on the fracture. The Mohr circle provides a useful tool allowing the visualization of these relationships. This construction determines the range of fracture orientations that are able to open, as well as determining the opening direction of these fractures. This is then used to produce ratios of the magma pressure and the principal stresses for some dykes from the Lizard ophiolite, U.K. © 1997 Elsevier Science Ltd

INTRODUCTION

The upper crust is pervaded by fractures which provide planes for the fluids to exploit. Dykes provide examples of such fluid flow and have been observed to intrude along pre-existing fractures (Currie and Ferguson, 1970; Roberts and Sanderson, 1971; Baer *et al.*, 1994; Jolly and Sanderson, 1995). In this Short Note, use is made of the Mohr circle, developed by Otto Mohr (1900, 1914), to examine the stresses and fluid pressures controlling fracture opening, following the analytical approach of Delaney *et al.* (1986). Thus, the wide range of stress and strain problems (e.g. Ramsay, 1967; Jaeger and Cook, 1969; Means, 1983; Passchier, 1986; Vissers, 1994) amenable to analysis by the Mohr circle is extended.

CONDITION FOR FRACTURE OPENING

For fluid to open a pre-existing fracture (Fig. 1), the fluid pressure (P_f) must exceed the normal stress (σ_n) acting on the fracture walls (Delaney *et al.*, 1986):

$$P_f \geq \sigma_n. \tag{1}$$

For this condition to be met, the stress on the fracture plane must lie in the shaded area of Fig. 2. The normal stress acting on a fracture (Fig. 1) can be expressed in terms of the fracture orientation (θ), and the maximum (S_H) and minimum (S_h) principal stresses:

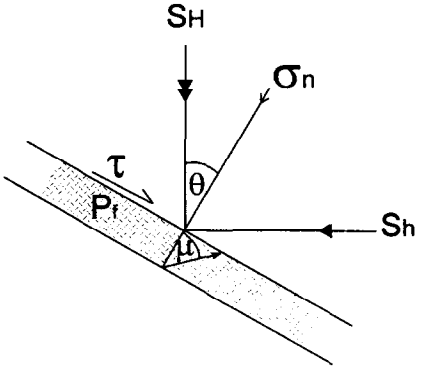

Fig. 1. The notation used for the analysis of fluid dilating a fracture. Compressive stresses are positive. The arrow indicates the opening direction of the fracture.

$$\sigma_n = \frac{S_H + S_h}{2} + \frac{S_H - S_h}{2}\cos 2\theta. \tag{2}$$

Delaney *et al.* (1986) derive the driving stress ratio (R) by substituting equation (2) in equation (1) and rearranging:

$$R = \frac{P_f - \frac{S_H + S_h}{2}}{\frac{S_H - S_h}{2}} \geq \cos 2\theta. \tag{3}$$

This is more clearly expressed in terms of the mean stress (σ_m) and the maximum shear stress (τ_{max}):

$$R = \frac{P_f - \sigma_m}{\tau_{max}} \geq \cos 2\theta. \tag{4}$$

Parameter R has been termed the driving stress ratio (Delaney *et al.*, 1986), and illustrates the role of fluid

* Present address: Department of Geology, Imperial College of Science and Technology, Royal School of Mines, Prince Consort Road, London SW7 2BP, U.K.

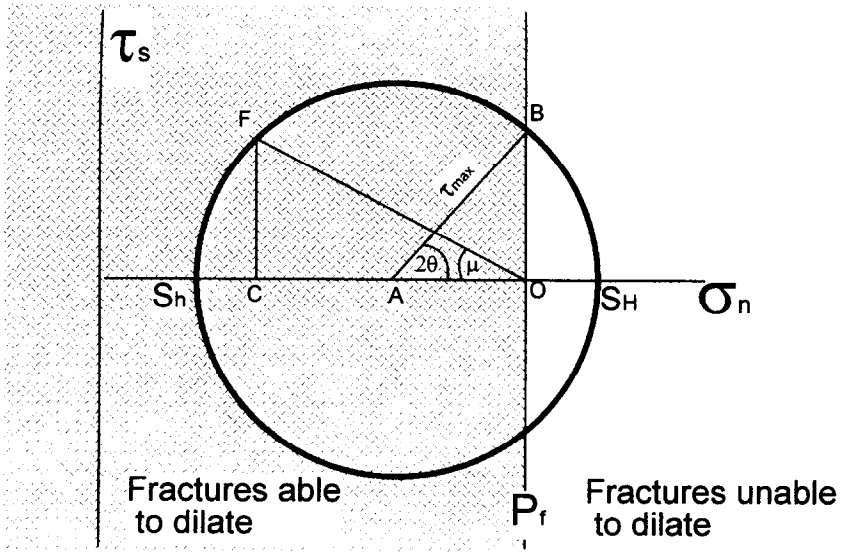

Fig. 2. A Mohr circle construction showing the maximum shear stress (τ_{max}), minimum principal stress (S_h) and maximum principal stress (S_H). The fluid pressure (P_f) is plotted along the normal stress (σ_n) axis. Fractures to the left of the fluid pressure line, the shaded area, are able to dilate as the normal stress is less than the fluid pressure. Fractures to right of the fluid pressure line are unable to dilate. The triangle *AOB* is used in the derivation of the *R* ratio (see text for details), and the triangle *FOC* establishes the opening direction (μ) of a fracture (see text for details).

pressure (P_f), mean stress (σ_m) and the maximum shear stress (τ_{max}) in determining conditions of fracture opening. *R* can be easily derived from the Mohr circle (Fig. 2), by considering the triangle *AOB*. The length *AO* can be expressed in two ways: first, in terms of the fluid pressure (P_f) and the mean stress (σ_m) (equation 5); and, second, in terms of the maximum shear stress (τ_{max}) and the fracture orientation (θ) (equation 6):

$$AO = P_f - \sigma_m \tag{5}$$

$$AO = \tau_{max} \cos 2\theta. \tag{6}$$

Combining equations (5) and (6) gives

$$P_f - \sigma_m \geq \tau_{max} \cos 2\theta. \tag{7}$$

Clearly, from Fig. 2, the following relationships apply: when $P_f < S_h$, no fractures open ($R < -1$); when $S_h < P_f < S_H$, a limited range of fracture orientations are able to open ($1 > R > -1$); when $P_f > S_H$, fractures of any orientation can open ($R > 1$).

OPENING DIRECTIONS

Having established a simple Mohr construction to determine the orientations of fractures that are able to open, it is now necessary to establish the opening directions of these fractures. Delaney *et al.* (1986) express the opening direction (μ) in terms of shear stress (τ), normal stress (σ_n) and the fluid pressure (P_f) (Fig. 1) as follows:

$$\tan \mu = \frac{\tau}{P_f - \sigma_n} = \frac{\sin 2\theta}{R - \cos 2\theta}. \tag{8}$$

This may be determined directly from the Mohr circle for any stress which satisfies the conditions for opening (such as *F* in the shaded area in Fig. 2). Consider the triangle *FOC* (Fig. 2), in which the length $FC = \tau$ (shear stress), and the length $CO = P_f - \sigma_n$ (difference between fluid pressure and normal stress). It follows from equation (8) that the angle *FOC* is the opening direction (μ). Note that for the limiting condition for opening (point *B*), $\mu = 90°$; i.e. opening is parallel to the fracture.

MOHR CIRCLE CONSTRUCTION IN THREE DIMENSIONS

The mechanics of dyke opening in two dimensions can easily be extended to three dimensions using the Mohr circle construction, the conditions for opening again being represented by the shaded area in Fig. 3.

Baer *et al.* (1994) have extended the two-dimensional approach of Delaney *et al.* (1986) to three dimensions. They introduce two terms to describe the relationship between the fluid pressure and the principal stresses, the driving pressure ratio (R') and the stress ratio (Φ). The stress ratio describes the relative magnitudes of the principal compressive stresses ($\sigma_1 \geq \sigma_2 \geq \sigma_3$) (Angelier, 1984; Baer *et al.*, 1994):

$$\Phi = \frac{\sigma_2 - \sigma_3}{\sigma_1 - \sigma_3}. \tag{9}$$

The driving pressure ratio (R') describes the magnitude of the fluid pressure relative to the maximum and minimum principal stresses (Baer *et al.*, 1994) (equation 8):

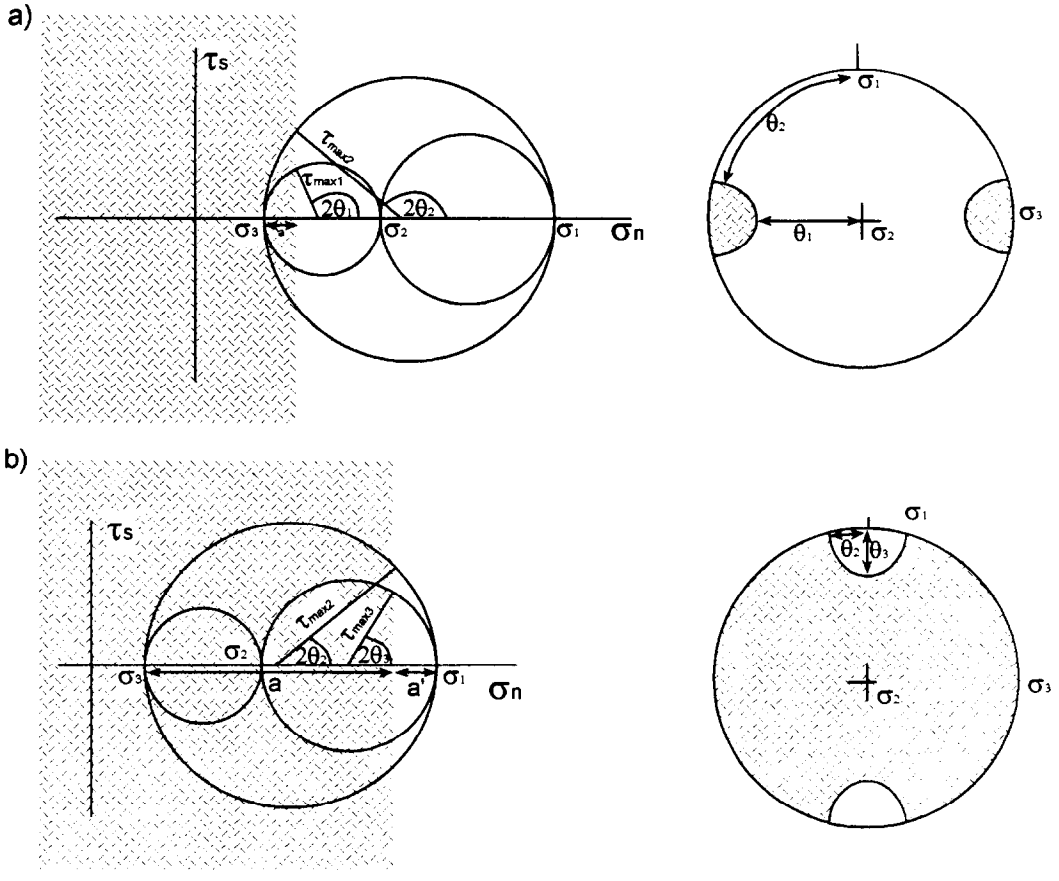

Fig. 3. (a) The conventions used for a three-dimensional Mohr circle when the fluid pressure (P_f) is less than the intermediate stress (σ_2). This produces a clustered distribution of poles to fracture wall, for fractures that open, about the σ_3 orientation on the stereogram, the shaded area. Also shown are the terms, length a, the maximum shear stresses (τ_{max1} and τ_{max2}) and the θ angles (θ_1 and θ_2), needed to derive the Mohr circle from a stereogram, see text for details. (b) The conventions used for a three-dimensional Mohr circle when the fluid pressure (P_f) is greater than the intermediate stress (σ_2). This produces a girdle distribution about the σ_1 orientation, the shaded area on the stereogram. Also shown are, lengths a and a', the maximum shear stresses (τ_{max2} and τ_{max3}) and the θ angles (θ_2 and θ_3), needed to derive the Mohr circle from a stereogram; see text for details.

$$R' = \frac{P_f - \sigma_3}{\sigma_1 - \sigma_3}. \tag{10}$$

R' differs from the R ratio of Delaney *et al.* (1986) in that it compares P_f with σ_3 rather than the mean stress (σ_m). For $R' < 0$, no fractures open; for $R' > 0$ fractures can open, the range of orientations depending on the stress ratio Φ (see Baer *et al.*, 1994 for details).

The range of fractures that are able to open can be more easily determined directly from the Mohr circle by using the angles θ_1, θ_2 and θ_3 in Fig. 3, but it is necessary to be careful with the conventions used. If the fluid pressure is less than the intermediate stress, then the angles θ_1 and θ_2 define the cluster of poles to fracture walls, measured within the relevant plane; for example θ_1 is measured in the σ_2–σ_3 plane (Fig. 3a). If the fluid pressure is greater than σ_2 then the angles θ_2 and θ_3 determine the girdle distribution of poles to fracture wall (Fig. 3b).

Figure 4 shows the range of orientations of fractures that are able to open as the fluid pressure increases from σ_3 to σ_1. At low fluid pressures (P_f close to σ_3), these form a clustered distribution, normal to the minimum principal stress. At higher fluid pressures (P_f close to σ_2) they form a girdled distribution, normal to the maximum principal stress (σ_1). When the fluid pressure reaches the maximum principal stress (σ_1), all orientations of fractures are able to open.

If the range of θ angles utilized by dykes or veins can be determined, then the analysis can be worked in reverse to determine the relative values of the stress and fluid pressure, through the parameters R' and the stress ratio (Φ) (Baer *et al.*, 1994). Using Fig. 3(a), the length $a = P_f - \sigma_3$ can be defined in terms of both θ_1 and θ_2:

$$a = \tau_{max1}(1 + \cos 2\theta_1) \tag{11}$$

and

$$a = \tau_{max2}(1 + \cos 2\theta_2). \tag{12}$$

Therefore, for $P_f < \sigma_2$, the stress ratio (Φ) can be expressed as:

$$\Phi = \frac{\sigma_2 - \sigma_3}{\sigma_1 - \sigma_3} = \frac{\tau_{max1}}{\tau_{max2}} = \frac{1 + \cos 2\theta_2}{1 + \cos 2\theta_1}. \tag{13}$$

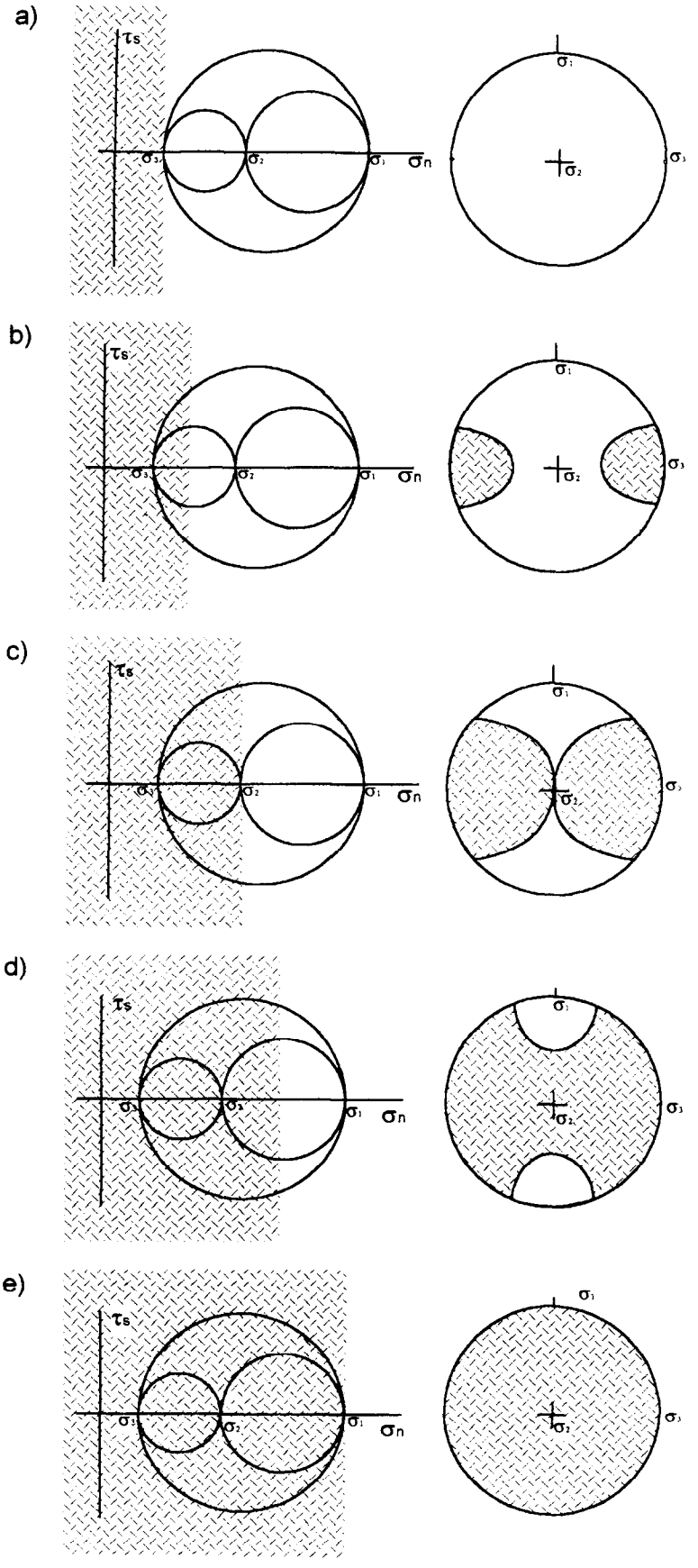

Fig. 4. The evolution of the Mohr circles and stereograms as there is a relative increase of the fluid pressure from (a) $P_f = \sigma_3$, to (b) $\sigma_3 < P_f < \sigma_2$, to (c) $P_f = \sigma_2$, to (d) $\sigma_2 < P_f < \sigma_1$, to (e) $P_f > \sigma_1$. The shaded areas on the stereograms are the predicted area of poles to dyke walls.

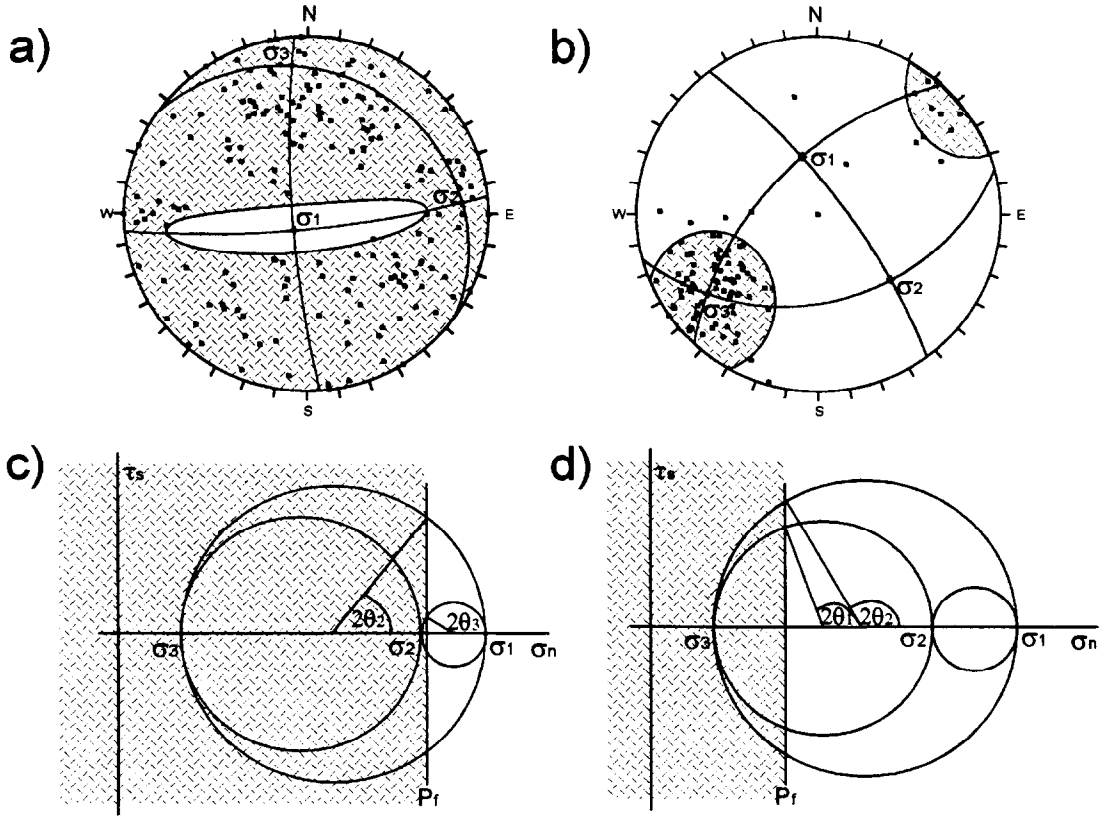

Fig. 5. (a) The sterogram of poles to dyke wall of the gabbro dykes from the Lizard ophiolite, Cornwall, U.K. The shaded area indicates the orientations of fractures that the fluid is able to dilate. (b) The sterogram of poles to dyke wall of the type II dykes from the sheeted dyke complex of the Lizard ophiolite. The shaded area indicates the orientations of fractures that the fluid is able to dilate. (c) The Mohr circle for the gabbro dykes producing a stress ratio (Φ) of 0.81 and a driving pressure ratio (R') of 0.82, calculated from the gabbro dyke orientation data. (d) The Mohr circle for the type II dykes producing a stress ratio (Φ) of 0.76 and a driving pressure ratio (R') of 0.25.

By a similar argument, for $P_f > \sigma_2$, and using the length $a' = \sigma_1 - P_f$ (Fig. 3b), the stress ratio (Φ) can be expressed in terms of θ_2 and θ_3:

$$a' = \tau_{max2}(1 - \cos 2\theta_2) \tag{14}$$

and

$$a' = \tau_{max3}(1 - \cos 2\theta_3). \tag{15}$$

Therefore, for $P_f > \sigma_2$, the stress ratio (Φ) can be expressed as:

$$\Phi = \frac{\sigma_2 - \sigma_3}{\sigma_1 - \sigma_3} = \frac{\tau_{max1}}{\tau_{max2}} = \frac{\tau_{max2}}{\tau_{max2}} - \frac{\tau_{max3}}{\tau_{max2}} = 1 - \frac{1 - \cos 2\theta_2}{1 - \cos 2\theta_3}. \tag{16}$$

This stress ratio (Φ) defines the form of the stress ellipsoid (Bott, 1959; Angelier, 1984; Baer *et al.*, 1994). It is this ratio, rather than the magnitudes of the principal stresses, which is determinable from kinematic data (as in most 'palaeostress' analysis methods).

The driving pressure ratio (R'), can be obtained by substituting $(\sigma_1 - \sigma_3) = 2\tau_{max2}$ and equation (12) in equation (10):

$$R' = \frac{P_f - \sigma_3}{\sigma_1 - \sigma_3} = \frac{a}{2\tau_{max2}} = \frac{(1 + \cos 2\theta_2)}{2}. \tag{17}$$

APPLICATION OF THE MOHR CIRCLE CONSTRUCTION

The Mohr circle construction is now applied to dykes from the Lizard ophiolite complex, Cornwall, U.K. Four dykes sets have been identified at various depths and stages in the development of the ophiolite (Roberts *et al.*, 1993; Jolly, 1996), on the basis of geochemistry, orientation and the timing of intrusion of the dykes relative to the extensional faulting. In this application of the Mohr circle construction we will concentrate on the gabbro dykes and the type II dykes, as defined by Roberts *et al.* (1993). The orientations of the dykes were recorded where they intersected traverse lines, these being oriented orthogonally and at oblique angles to each other to fully sample all orientations of dykes.

The gabbro dykes intrude the tectonized peridotite close to the petrological Moho, at Coverack (see fig. 1 of Roberts *et al.*, 1993). They are planar in form, have a wide range of orientations (Fig. 5a) and often intersect each other. There appears to be a lack of sub-horizontal dykes, which is not attributable to any sampling bias. This implies that the maximum principal stress was vertical, with the poles to the dykes forming a girdle distribution normal to this vector (see Fig. 4).

The type II dykes form the bulk of the sheeted dyke complex with the Lizard ophiolite. They are plagioclase–phyric dolerites and have a more evolved geochemistry than the gabbro dykes (Roberts *et al.*, 1993), and can be found predominantly between Porthoustock and Manacle point (Roberts *et al.*, 1993, fig. 1). The dykes have a high degree of alignment (Fig. 5b), the poles to the dyke walls clustering sub-horizontally NE–SW, indicating steeply dipping dykes trending NW–SE.

From Fig. 4, the principal stress axes can be located from the symmetry of the poles to dykes. To determine the symmetry axes, Bingham statistics (see Mardia, 1972) were applied to the gabbro and type II dykes, and from the resulting eigenvectors the angles of θ were established. In the case of the gabbro dykes, the magma pressure clearly exceeds the intermediate principal stress, as the poles to the dyke walls form a girdle distribution (Fig. 5a). The stress and driving pressure ratios are therefore calculated, using θ_2 and θ_3. The poles of the type II dykes form a clustered distribution (Fig. 5b), implying that the magma pressure is less than the intermediate stress. The stress and driving pressure ratios were calculated using θ_1 and θ_2. Substitution of these estimates of θ angles into equations (13), (16) and (17) returns a stress ratio of 0.81 and a driving pressure ratio of 0.82 for the gabbro dykes, and 0.76 and 0.25, respectively, for the type II dykes.

CONCLUSIONS

This Mohr circle construction provides a useful tool for the analysis of dykes and veins in allowing the relative fluid pressure and principal stress magnitudes to be estimated graphically. The two-dimensional method is easily extended to three dimensions using the Mohr circle. Worked examples using dykes from the Lizard ophiolite illustrate the power and simplicity of this approach.

Acknowledgements—This work was carried out while Richard Jolly was in receipt of a studentship at the University of Southampton. S. H. Treagus, W. D. Means and an anonymous reviewer are thanked for their helpful comments.

REFERENCES

Angelier, J. (1984) Tectonic analysis of fault slip data sets. *Journal of Geophysical Research* **89**, 5835–5848.

Baer, G., Beyth, M. and Reches, Z. (1994) Dikes emplaced into fractured basement, Timna Igneous Complex, Israel. *Journal of Geophysical Research* **99**, 24039–24051.

Bott, M. H. P. (1959) The mechanics of oblique slip faulting. *Geological Magazine* **96**, 109–117.

Currie, K. L. and Ferguson, J. (1970) The mechanism of intrusion of lamprophyre dikes indicated by 'offsetting' of dikes. *Tectonophysics* **9**, 525–535.

Delaney, P. T., Pollard, D. D., Zioney, J. I. and McKee, E. H. (1986) Field relations between dikes and joints: Emplacement processes and paleostress analysis. *Journal of Geophysical Research* **91**, 4920–4938.

Jaeger, J. G. and Cook, N. W. G. (1969) *Fundamentals of Rock Mechanics*. Methuen, London.

Jolly, R. J. H. (1996) Mechanisms of igneous sheet intrusion. Ph.D. thesis, University of Southampton.

Jolly, R. J. H. and Sanderson, D. J. (1995) Variations in the form and distribution of dykes in the Mull swarm, Scotland. *Journal of Structural Geology* **17**, 1543–1557.

Mardia, K. V. (1972) *Statistics of Directional Data*. Academic Press, London.

Means, W. D. (1983) Application of the Mohr circle construction to problems of inhomogeneous deformation. *Journal of Structural Geology* **5**, 279–286.

Mohr, O. (1900) Welch Umstände bedingen die Elastizitätsgrenze und den Bruch eines Materials? *Zeitschrift Verein Deutsch Ingenieur* **44**, 1524–1530; 1572–1577.

Mohr, O. (1914) *Abhandlugen aus dem Gebiete der technische Mechanik*, 2nd edn. Ernst und Sohn, Berlin.

Passchier, C. W. (1986) The use of Mohr circles to describe non-coaxial progressive deformation. *Tectonophysics* **149**, 323–338.

Ramsay, J. G. (1967) *Folding and Fracturing of Rocks*. McGraw-Hill, New York.

Roberts, J. L. and Sanderson, D. J. (1971) The intrusive form of some basaltic dykes showing flow lineation. *Geological Magazine* **108**, 489–499.

Roberts, S., Andrews, J. R., Bull, J. M. and Sanderson, D. J. (1993) Slow-spreading ridge axis tectonics: Evidence from the Lizard complex, UK. *Earth and Planetary Science Letters* **116**, 101–112.

Vissers, R. L. M. (1994) Finite strain in simple shear, inspected with Mohr circles for stretch. *Journal of Structural Geology* **16**, 1723–1726.